Magnetic circular dichroism in resonant x-ray emission from impurities: Results at the $L_{2,3}$ edges of Mn in Ni

F. Borgatti,[1] P. Ferriani,[2] G. Ghringhelli,[3,4] A. Tagliaferri,[4,3] B. De Michelis,[4] C. M. Bertoni,[2] N. B. Brookes,[3] and L. Braicovich[4]

[1]*INFM-OGG at the ESRF, European Synchrotron Radiation Facility, B.P. 220, F-38043 Grenoble Cédex, France*
[2]*INFM-Dipartimento di Fisica, Università di Modena e Reggio Emilia, via Campi 213/a, I-41100 Modena, Italy*
[3]*ESRF, European Synchrotron Radiation Facility, B.P. 220, F-38043 Grenoble Cédex, France*
[4]*INFM-Dipartimento di Fisica, Politecnico di Milano, Piazza Leonardo da Vinci 32, I-20133 Milano, Italy*

We present a study of Mn magnetic impurities (about 2%) in Ni with resonant x-ray emission spectroscopy excited at the $L_{2,3}$ edges of Mn using circularly polarized x rays incident almost parallel/antiparallel to the magnetization. The results are discussed jointly with absorption magnetic circular dichroism and complemented with elastic reflectivity measurements. Moreover, we show that emission spectroscopy is particularly suitable to the impurity problem, since the self-absorption/saturation corrections to the measurements are rather limited. The problem is treated also theoretically with a full multiplet splitting calculation of a single Mn^{2+} ($3d^5$) ion with cubic crystal field. The theory reproduces satisfactorily all experimental trends of the features dispersing with the incident photon energy in the whole L_3 region, whereas it is not adequate just below the L_2 excitation. The joint use of the theory and of the measurements allows us to extract the nondispersive component from the measured spectra. It is shown that this component does not correlate directly with the $3d$-Mn local density of states. The general implications of the results are discussed.

I. INTRODUCTION

During the last decade the magnetic circular dichroism (MCD) in core absorption and in photoemission has become a central issue in the spectroscopy of magnetic systems. On the other hand, the study of magnetic systems with x-ray *emission* spectroscopy has not been exploited much since the initial theoretical suggestion by Strange *et al.*[1] and the experimental work of Refs. 2–7. More recent experimental work has been published by Duda[8] and by Yablonskikh *et al.*[9,10] while theoretical work has been done by Jo and Parlebas.[11] This relatively limited development is due to a variety of difficulties in emission MCD, as is apparent from the literature and as will be shown below. In the present work we address the study of magnetic impurities with resonant emission. This topic is very convenient to emission spectroscopy. In fact, in concentrated samples the penetration depth of the radiation is very much dependent on the photon polarization. This is due to the strong absorption MCD so that the distortion of the emission spectra due to self-absorption/saturation is dramatic as shown in Refs. 5 and 7. This is not the case in dilute systems where the majority component dominates with its nondichroic absorption. Real experiments on dilute systems based on third generation synchrotron radiation sources approach this limit and the corrections are definitely tolerable as shown here.[12]

In this field, we have chosen Mn diluted in Ni, which is a prototypical case of magnetic impurity having a high magnetic moment. Moreover, electronic state calculations for the ground state are available.[13]

The emission experiments consist in the excitation with circularly polarized light (photon energy $h\nu_{in}$) incident almost parallel/antiparallel to the magnetization and with $h\nu_{in}$ tuned at selected convenient values. The emission spectrum *vs* the outgoing photon energy $h\nu_{out}$ is measured at a convenient angle, without measuring the polarization of the emitted radiation.[14] In the present case we use the Mn channel $2p^6 3d^n \rightarrow 2p^5 3d^{n+1} \rightarrow 2p^6 3d^n$ where n is the $3d$ occupation in the ground state (i.e., we study resonant valence excitation via an L hole). This process results in spectra containing a nondispersive contribution and a component dispersing with the incident photon energy, which is usually called a Raman component and typical of resonant Raman scattering (RRS). Thus the dispersive component shows the features appearing at constant energy loss corresponding to the excitation energy of the sample in the final state. The emission MCD is the difference between the spectra (measured vs $h\nu_{out}$) with opposite circular polarizations of the incident light. Due to the polarization of the core hole created in the absorption this emission MCD should be related, accordingly to the initial suggestion by Strange *et al.*,[1] to the energy distribution of the spin unbalance of the occupied states. However, the situation is far more complicated as it is apparent from the literature (in particular, see Ref. 8) and as we will show here. In the present work we concentrate on the resonant effects since the excitation well above threshold (possible also with polychromatic radiation as in Ref. 2) involves complicated processes connected with multiple excitations (see Refs. 2 and 8), so that the interpretation is very indirect. In the resonant excitation we pay particular attention to the L_3 case, simpler because the Coster-Kronig (CK) channel converting the L_2 into an L_3 hole is in itself dichroic, as shown already in Ref. 4 and rationalized by Jo and Parlebas.[11]

In the present work, besides the emission spectra, we have measured also resonant elastic reflectivity in specular geometry and we use the results jointly. In particular the reflectiv-

ity is used to obtain information on the absorption MCD, which is fitted together with the emission with a model based on the Kramers-Heisenberg (KH) formula for the calculation of the cross section.

Besides the relevance of showing that magnetic impurities are particularly appropriate for the emission experiments, the main points presented here can be anticipated as follows.

(i) The importance of the interplay between reflectivity and emission measurements is pointed out.

(ii) The relevance of the dispersive component in the emission spectra of Mn impurities is shown. This is in broad sense analogous to what happens in other Mn compounds as pointed out recently by the results of Ref. 8 on the $Ni_{75}Mn_{10}Al_{15}$ alloy and of Ref. 9 on NiMnSb and Co_2MnSb.

(iii) The possibility of describing satisfactorily the dispersive component with the results of a KH calculation based on an ionic model, a result far from being obvious in a metallic system as the present one.

(iv) The absence of a straightforward correlation between the nondispersive component and the local density of $3d$ states of Mn. This is important since it is opposite to the initial suggestion by Strange[1] and shows limitations in the use of emission dichroism to explore the spin unbalance of the occupied states.

The paper is organized as follows. The experimental and theoretical methods are given in Secs. II A and II B. The results on the resonant emission are given in Sec. III, while the reflectivity data and the MCD information are given in Sec. IV. The self-absorption/saturation effect and the dilute limit are briefly discussed in Sec. V. The theoretical results are summarized in Sec. VI and are compared with the experiment in the discussion given in Sec. VII. The conclusions are given in Sec. VIII.

II. METHODS

A. Experiment

The measurements were made at the beam line ID12B (Ref. 15) of the European Synchrotron Radiation Facility (ESRF – Grenoble). The beam line, based on the helical undulator Helios I,[16] delivered circularly polarized radiation (80% at the energy of the present experiment). The measurements were done with a system consisting of a dedicated monochromator[17] used to prepare the beam incident onto the sample and of a spectrograph measuring the emission spectra.[18] The magnetizing system is described in Ref. 19; the magnetic field was 0.2 T which was sufficient to approach saturation within 5%. The angle between the incident and the scattered momentum is 110° as shown in the inset in the lower panel of Fig. 1. This angle is chosen to have the emission nearly normal to the magnetization (incidence at 15° from the surface and emission at 5° from the normal). This avoids dichroic effects in self-absorption along the emission path. The incident bandpass was 1 eV and the energy bandpass of the analyzing spectrograph was 0.8 eV. The relative signs of the polarization and of the magnetization were changed cyclically every 5 min to minimize the effect of possible drifts. In the reflectivity measurements, the sample was rotated to have specular reflection and the mea-
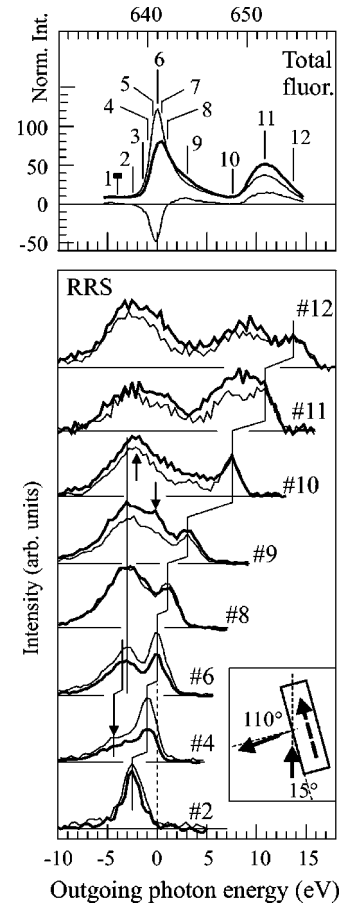

FIG. 1. A selection of measured emission spectra (raw data) of magnetic Mn impurities in Ni (lower panel) measured vs the outgoing photon energy $h\nu_{out}$ with excitation at selected incident energies $h\nu_{in}$. The excitation energies are given by the arrows along the Mn total fluorescence curves vs $h\nu_{in}$ given in the upper panel together with the difference spectrum. The thick and the thin lines refer to opposite orientation of the incident helicity vector and of the sample magnetization. The geometrical arrangement is given by the sketch in the inset (lower panel). The energies are measured conventionally from the L_3 peak. The absolute energies are in the upper panel.

surements were normalized to the incident flux measured with the photocurrent from a semitransparent Al film. All measurements were done at room temperature. The total fluorescence was measured with a photodiode.

The sample was grown in a separate preparation chamber by co-evaporation of Ni and Mn onto polished Si(100) substrates by electron bombardment from independent evaporators. The base pressure in the evaporation chamber was below 2×10^{-10} mbar and raised in the lower 10^{-9} range during the evaporation. The deposition rate (monitored with a quartz microbalance) was sufficiently high that the contamination during growth was negligible. The total thickness of the samples was about 1800 Å. Shutters were available to monitor the rate of each single evaporator and to cover the sample, when needed. Great care was taken to check the stability of the system in order to avoid composition inhomogeneities. The preparation of one sample needed typically

90 min and the rates of Ni and Mn were tested every 15 min (this required about 30 sec). Several samples were grown in order to select the best for the experiment. During each growth, two targets were installed side by side in order to produce two strictly equivalent samples, one for the characterization and the other for the emission experiment. The samples were capped with a thin Au overlayer to prevent contamination from the residual gas when stored in vacuum.

The samples could be extracted from the preparation chamber with a transfer arm and inserted in the measurement chamber without going to air. The replica sample was dismounted and inserted (less than 3 min in air) into an x-ray photoemission spectroscopy (XPS) scanning Auger system. The composition was verified with core XPS and a quantitative depth profiling was done in several locations with an Auger system having 2000-Å lateral resolution. The locations of the depth profiles were decided by using the Auger system as a scanning microscope. The Mn concentration is well below the solubility limit and this ensures a good bulk homogeneity as tested by depth profiling. We have also found surface segregation of Mn as expected from the vapor pressures. Typically in the first five layers (about 10 Å), Mn is the majority component. This has negligible effects in our bulk sensitive emission experiment even when the incidence is at 15° from the surface. The enriched region has typically a weight of 1% of the emission spectra, even at grazing incidence. On the other hand, Mn segregation prevents any quantitative measurements of the absorption dichroism with total electron yield, due to its high surface sensitivity. Finally, XPS Auger analysis did not show any evidence of oxidation.

B. Theoretical method

The calculations have been done in a purely ionic approximation whose merits and limitations are discussed in Secs. VI and VII. The impurity is described in a single configuration all-electron picture, with Mn^{2+} $(3d^5)$ in a cubic crystal field. The contributions to the spectrum dispersing with $h\nu_{in}$, i.e., the Raman contribution $S_{disp}(h\nu_{in}, h\nu_{out})$, is calculated as a second-order process using the Kramers-Heisenberg (KH) formula with the delta function giving the total-energy conservation smeared into a Lorentzian.

$$S_{disp}(h\nu_{in}, h\nu_{out}) \approx \sum_f \left| \sum_i \frac{\langle f|T^{(e)}|i\rangle \langle i|T^{(a)}|g\rangle}{E_g + h\nu_{in} - E_i - i\Gamma_i} \right|^2$$

$$\times \frac{\Gamma_f/\pi}{(E_g + h\nu_{in} - E_f - h\nu_{out})^2 + \Gamma_f^2}, \quad (1)$$

where $|g\rangle$, $|i\rangle$, and $|f\rangle$ are the initial, the intermediate, and the final states with energies E_g, E_i, and E_f, respectively. In the formula we have omitted the multiplicative constants and the very slow varying factor (ν_{out}/ν_{in}). The configurations in the ground and intermediate state are $3d^5$ and $2p^5 3d^6$, respectively, and the final configuration is again $3d^5$. In the initial state all multiplet terms of $3d^5$ are considered and weighted with a Boltzmann factor, so that the calculation is temperature dependent. The results depend on the

ratio $T_R = (k_B T/\Delta E_{exch})$ where ΔE_{exch} is the exchange splitting between two neighboring levels of the magnetic ground state. Hereafter T_R will be called "reduced temperature." Since no independent experimental determination of ΔE_{exch} is available, we treat T_R as a parameter to be determined in the fitting of the experimental results. Of course, a value of T_R implies a value of ΔE_{exch} since the experiment is done at a known temperature (300 K). Thus one has to test *a posteriori* if the value of ΔE_{exch} is in a reasonable range. In the final state all multiplet terms are accounted for. Since the outgoing polarization is not observed, the intensities are summed over the polarizations of the scattered beam. The matrix elements and all the Slater integrals are calculated by the Hartree-Fock method with relativistic corrections.[20] As usual, the integrals are rescaled to take approximately into account the part of the intra-atomic correlation not included in the Hartree-Fock treatment. The reduced temperature, the rescaling factor and the crystal field were optimized in the joint fit of the absorption and of the emission spectra. The reflectivity results were used to calibrate the measured absorption MCD as explained below (Sec. IV). As shown in Sec. VI the best results from the joint fitting of emission and absorption are obtained with $T_R = 1.5$, $10Dq = 0.7$ eV, and a rescaling of the F and G Slater integrals to 75%.

III. EXPERIMENTAL RESULTS ON RESONANT EMISSION

The emission spectra have been measured at selected excitation energies $h\nu_{in}$, spanning from below the Mn-L_3 threshold to above the L_2 absorption peak. The excitation energies $h\nu_{in}$ labeled from 1 to 12 are indicated in the upper panel of Fig. 1 giving the total fluorescence yield curves of magnetic Mn impurities measured with the two opposite circular polarizations and their difference. It is known from Refs. 3 and 4 and in more detail from Ref. 21 that the total fluorescence yield curves cannot give reliable quantitative information on absorption MCD. Nevertheless, they are useful since they mimic roughly the absorption spectra and are easily measured with the diode detector as explained above. In the figure, the spectra are normalized so that the L_3 peak averaged over the polarization is equal to 100. The emission results, i.e., the spectra vs the outgoing photon energy $h\nu_{out}$, are shown in the lower panel of Fig. 1 giving, for space reasons, a subset of the results. The experiment shows a considerable emission dichroism having a strong dependence on the excitation energy $h\nu_{in}$. In Fig. 1 the energies of the photons are measured from the energy of the scattered elastic peak excited at the L_3 peak of Mn (case 6). This makes the reading of the relative shifts of the spectra easier. The absolute values of the energies are given at the top of the upper panel.

Some important features can be seen already in the raw data, even without comparing with theory.

(i) The elastic peak (dispersing with $h\nu_{in}$) has a clear dichroism that is maximum in the L_3 region.

(ii) A clear shoulder at about 3.5 eV below the elastic peak is seen with excitations 4 and 9 (arrows in the figure). This dispersive inelastic contribution is due to transitions to lower spin in the final state in analogy to what was demon-

strated in MnO by Butorin *et al.*[22] (hereafter this loss will be called "lower spin excitation"). This excitation is seen also in $Ni_{75}Mn_{10}Al_{15}$ (Ref. 8) and probably also in Co_2MnSb.[9] The assignment to lower spin is confirmed by the calculations given in the present paper.

(iii) The sign of the emission MCD is the same as the absorption MCD with a change around excitation 8, i.e., at the zero crossing of MCD. At this excitation energy the dichroism integrated along $h\nu_{out}$ is close to zero while the spectral distribution gives two regions with small and opposite dichroism.

(iv) When $h\nu_{in}$ increases above the zero crossing of the absorption MCD there is a clear transfer of the emission dichroism from the elastic peak to the lower spin excitation. These results have a counterpart in what was found for $Ni_{75}Mn_{10}Al_{15}$ alloy[8] and probably for Co_2MnSb.[9]

(v) As seen immediately in spectra from 6 to 9 the RRS spectra contain a nondispersive component shown by the solid vertical line in Fig. 1 at about $h\nu_{out} = -3$ eV. In particular the spectra 6 are likely to contain a superposition of dispersive and nondispersive contribution. This is confirmed by the analysis given in Sec. VII. The dichroism of the non-dispersive contribution is strong and has the same sign of the absorption MCD.

(vi) In case 10, i.e., with the excitation immediately below the L_2 threshold (i.e., well above L_3), the low-energy peak is not at the energy of the nondispersive component as shown by an arrow. This loss corresponds to an excitation in the final state at least around 8 eV (see also Sec. VIII).[23]

(vii) With excitation in the L_2 region, a strong Coster-Kronig (CK) contribution is seen. The CK conversion is polarization dependent as known from the literature.[4,11] The study of this problem in the impurity regime in a metallic system is premature so that the L_2 spectra will be not discussed and are presented for completeness.

IV. EXPERIMENTAL RESULTS ON SPECULAR REFLECTIVITY AND ABSORPTION MAGNETIC CIRCULAR DICHROISM

As anticipated above the Mn segregation does not allow the absorption MCD to be measured from electron yield. This can be used to give the *shape* of MCD vs $h\nu_{in}$, but not the absolute value. In fact, in the Mn enriched surface region, the Mn concentration is higher than 20% so that Mn is no more magnetic.[24,25] This gives a drastic reduction of the dichroism measured with total electron yield while the shape of the difference curve is safer because the contribution of the nonmagnetic Mn is canceled in the subtraction. On the other hand, the total fluorescence yield (Fig. 1) gives only a qualitative indication as it is well known.[21] Thus we used a different approach, i.e., we recovered MCD information from specular elastic reflectivity which is much less surface sensitive since it is a photon in – photon out measurement. This has been done as follows with an accuracy sufficient to the present purposes.

(i) After rotating the sample, we have measured the emission spectra in specular geometry (35° from the sample normal). The elastic peak is strongly enhanced as shown, e.g.,
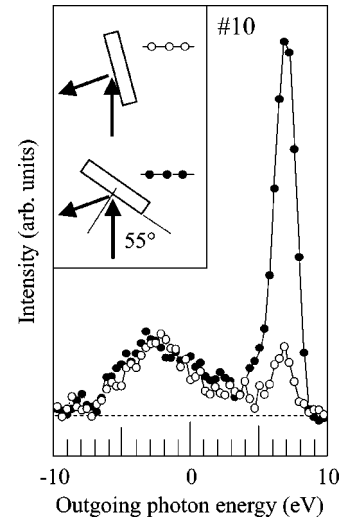

FIG. 2. Magnetic Mn impurities in Ni: the emission spectra summed over the polarizations and measured with the excitation 10 (see Fig. 1) in the two different geometrical arrangements shown in the inset. The open dots refer to the case of Fig. 1 and the black dots to the specular case.

with excitation 10 in Fig. 2. It is thus easy to obtain the elastic reflectivity at various $h\nu_{in}$ (normalizing to the incident photon flux). The results, summed over the incident polarization and with nonmagnetized sample, are given in Fig. 3 (lower panel, black dots).

(ii) We have measured the electron yield spectrum without magnetizing the sample and summing over the incident polarizations (Fig. 4, thin line in the upper panel).

(iii) We have done a first-principle calculation of the reflectivity, as in Ref. 26. To this end, the absorption is needed to determine the imaginary part of the refraction index. The absorption coefficient is synthesized as follows. The absorption coefficient in a wide energy range is obtained by combining the elemental absorption of Ni and Mn taken from the databases[27] and weighted by the composition. These data are accurate in the general trends but not in the resonant absorption around threshold (Mn-$L_{2,3}$ and Ni-$L_{2,3}$), which is very important for our analysis. These resonant parts have been taken from our electron yield measurements (as in Fig. 4 for Mn-$L_{2,3}$) by rescaling the measured spectra to the jump (known from the tabulated data[27]) from below threshold to well above the L_2 peak. The real part of the refractive index is obtained from a Kramers-Kronig transformation of the imaginary part. The calculated reflectivity, shown in the middle panel of Fig. 3, is in reasonable agreement with the experiment. This demonstrates that the shape of the absorption spectrum obtained with the electron yield of Fig. 4 and used in the calculation is realistic. Thus Mn segregation does not affect drastically the electron-yield spectra. The consistency of the two approaches makes it possible to use dichroic reflectivity to calibrate the MCD given by the electron yield.

(iv) The reflectivity MCD at the L_3 peak is shown by the open squares in the upper panel of Fig. 3. By using the theory of the polarized reflectivity as in Ref. 26, i.e., by inserting the polarization effects in the simulation of the reflectivity, we obtain the absorption MCD that is needed to
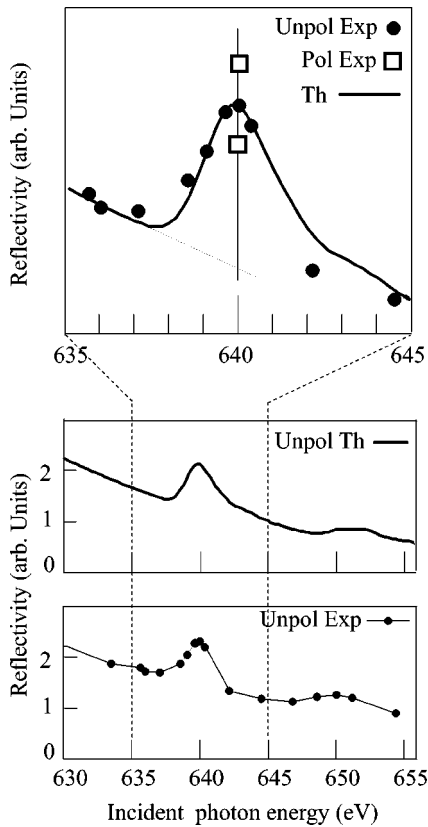
FIG. 3. Specular elastic reflectivity of Mn impurities in Ni vs the incident photon energy. The measurements summed over the polarizations are given in the lower panel and the calculated reflectivity in the middle panel. A blowup of the L_3 region is given in the upper panel including the measurements at L_3 with circularly polarized light and magnetized sample (open squares).
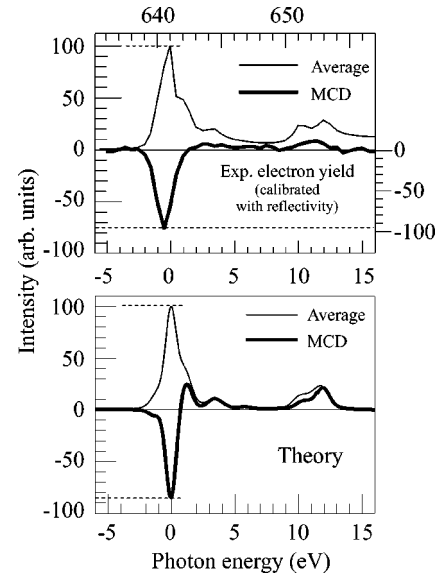

FIG. 4. $L_{2,3}$ absorption in magnetic Mn impurities in Ni. Upper panel: measurements with total electron yield averaged over the incident circular polarizations (thin line) and the absorption MCD (thick line). The calibration of the dichroism is done on the basis of the reflectivity as explained in detail in Sec. IV. The left scale refers to the raw data and the right scale takes into account the partial polarization of the incident beam. Lower panel: calculations done as explained in Secs. VI and VII.

give the measured reflectivity MCD. Thus we calibrate the difference curve measured with total electron emission. The result is the absorption MCD of the upper panel of Fig. 4 (heavy line). The left scale is not corrected for the incident polarization (80%) and the right scale accounts for it. After this correction, the peak absorption MCD is around 95%.

Given the numerous approximations in the analysis, the final evaluation of the MCD is affected by a non-negligible uncertainty. We have done an extensive numerical analysis of the sensitivity to all parameters and approximations obtaining an uncertainty of the absorption MCD up to $\pm 10\%$. Thus we will assume cautiously an L_3-peak absorption MCD between 85% and 105% with complete incident polarization. Of course, these uncertainties prevent sum rules to be used.

V. SELF-ABSORPTION/SATURATION PROBLEMS

As already stressed in the introduction, very strong corrections to the raw data are required in concentrated systems in order to recover the useful information on the scattering cross sections. This happens even when the emission direction is chosen almost normal to the magnetization, in order to avoid dichroic self-absorption. In fact, the penetration of the incident beam is dichroic and this gives anyhow different

exit paths generating strong artifacts in concentrated systems as shown in Ref. 7 and references quoted therein. On the other hand, in the extreme dilute limit, the absorption is dominated by the nondichroic absorption of the majority component and the problem does not exist. We have assessed this problem in the present case by making a calculation as in Ref. 7: these effects are largely tolerable. In the calculation we have used the absorption coefficient employed in the simulations of the reflectivity discussed in the previous section. With the exception of the excitation at the L_3 peak all corrections to the emission dichroism are below 10% and are almost independent of the outgoing photon energy (no distortion of the spectra). At L_3 the Mn contribution to the total absorption becomes non-negligible and the measured peak dichroism is multiplied by a factor about 0.7, again with very little dependence on the outgoing photon energy. A measurement at L_3 needing much smaller corrections, if any, would require concentrations around 0.1%, which are definitely below our concentration of 1.8–2%. The experimental feasibility at such low concentrations is not far from being reached at present, in consideration of the performances of the most recent synchrotron radiation beam lines.[28] Of course, this increases the interest of the present results. Hereafter we do not include these effects in the comparison between theory and experiment because already a straightforward comparison without corrections allows the main topics to be discussed. We believe that this approach is more transparent because we avoid using too many parameters. This is the great advantage of the work on impurities.

Similar arguments apply also to the total fluorescence spectra reported in Fig. 1 (upper panel) and confirms the

difficulties in extracting absorption MCD from total fluorescence even with concentration impurities around 1%.[29]

VI. THEORETICAL RESULTS

As anticipated above, we used a purely ionic model in the interpretation of the emission dichroism. This approximation might seem very poor for a metallic system like ours. As a matter of fact, it has been already shown that for Mn atoms dispersed in a metallic system the core excitation properties are dominated by atomiclike effects. Hence a full multiplet-splitting calculation (with a dominant $3d^5$ configuration) is a good starting point. In other words, this approach is not confined to the oxidelike cases. This relevant point has been pointed out in $L_{2,3}$ absorption from Mn chemisorbed on Fe(100).[30] In fact, the spectra are dominated by the local excitations that can be described rather well in an all-electron atomiclike picture. The extension of the ionic model to the present case is supported by our measured $L_{2,3}$ absorption spectrum (Fig. 4, upper panel), similar in shape to that given in Ref. 30 for Mn on Fe(100). These arguments are also consistent with what was suggested recently on resonant photoemission from thin Mn films by Richter *et al.*[31] We expect then the ionic approach to be a useful starting point for the interpretation of the emission spectra. This is the case already in the simplest application of the model based on a single configuration ($3d^5$) as shown in Sec. VII.

In a joint fitting of absorption and emission spectra we have found the best crystal field $10Dq = 0.7$ eV and the best reduced temperature $T_R = 1.5$ (see Sec. II B). This T_R corresponds to $\Delta E_{exch} = 17$ meV, which is an acceptable value within the range used routinely in the calculation of absorption MCD. The Slater integrals were rescaled by 75% that is a rather common rescaling factor.

With these parameters the absorption spectrum averaged over the polarizations and the absorption MCD are given in Fig. 4 (lower panel). The results of Fig. 4 refer to complete polarization of the incident beam and give an L_3-peak dichroism of 85%, which is at the lower edge of the experimental interval. As we will show this comes from a compromise with the fitting of the emission dichroism. The energy dependence of the absorption MCD is in general agreement with the experiment. The only inaccuracy in the MCD is found just above the zero crossing in the L_3 region. At present, it is not possible to assess the origin of this problem in consideration of the experimental uncertainties and of the simplified model.

Some of the calculated emission spectra are shown in Fig. 5 together with their dependence on the scattering angle. The KH formula gives the dispersive contribution and the results are plotted vs the energy transferred to the sample so that the elastic peak is at zero transferred energy. As pointed out above, a significant aspect of the emission measurements is the transfer, at increasing $h\nu_{in}$, of the dichroism from the elastic peak to the feature corresponding to lower spin final states. This trend is well reproduced by the theory (spectra at excitation 6 and 9 in Fig. 5) where we give calculations with 100% incident polarization without accounting for the finite bandpass of the experiment. We present calculations at two
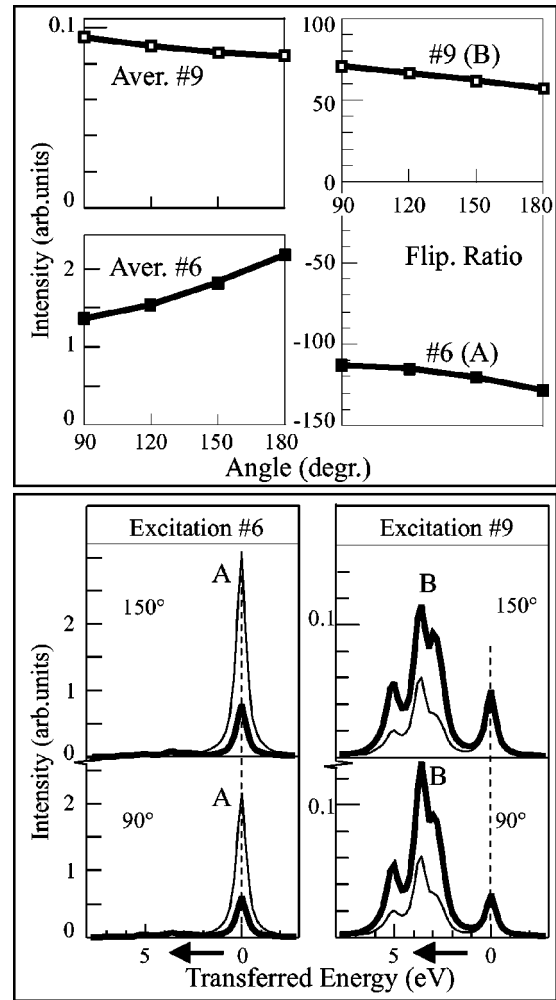

FIG. 5. Calculated scattering spectra from magnetic Mn impurities (Mn^{2+}-$3d^5$ ground state). The labels indicate the $h\nu_{in}$ energies given in the upper panel of Fig. 1 and the scattering angle is defined in the inset in Fig. 1 (lower panel). The spectra at two angles (90° and 150°) are given in the lower panel. The angular dependence of the peaks A and B is given in the upper panel (Aver = polarization averaged intensity (at the left) and flipping ratio at the right; for details see Sec. VI).

scattering angles (90 and 150°—note the expansion of the scale in case 9). With excitation to the intermediate lower spin states (case 9), the final states giving the feature B are coupled directly to the intermediate state without any further spin flip of any electron, as opposed to what happens in the elastic peak, where a further spin flip occurs. This explains qualitatively both the dominant intensity of the inelastic part and the transfer of the dichroism to the inelastic part. This argument is easily understood in cylindrical SO_2 symmetry, i.e., in the magnetic system without crystal field. When the crystal field is accounted for, the symmetry becomes C_{4h} with a reshuffling of the states. We have seen numerically that the crystal-field effect gives a further reduction of the dichroism at the elastic peak.[32]

The information on the angles is summarized in the upper panel of Fig. 5 giving the angle dependence of peaks A and B with the excitations 6 and 9. In the figure, we give the values

averaged over the incident polarizations and the percent dichroism with respect to the average value (flipping ratio). As specified above the experiment is carried out at a given angle (scattering at $110°$) dictated by technical constraints and by the need of minimizing the self-absorption/saturation. The theoretical angular dependence shows that the experiment, although done at an angle, is significant of the situation as a whole since the theoretical angular dependence is not strong.

VII. DISCUSSION

The comparison with the experiment requires to disentangle the dispersive and the nondispersive contributions. This is done here by using the theory and the experiment jointly. As we show in this section, the difference between the measured spectra and the theoretical dispersing spectrum gives a contribution which does *not* disperse and has *constant* shape when $h\nu_{in}$ is changed. In this way, we obtain the nondispersive component. We stress that the nondispersive behavior of the difference spectrum is a result of the analysis and not an assumption.

The nondispersive contribution has been obtained in cases 3 to 6 both in the polarized spectra and in the spectra summed over the polarizations, always with the same nondispersive spectrum within the accuracy of the measurements. The procedure is shown in Fig. 6 in cases 4 and 6 summed over the polarizations. In the lower panel, the black squares give the raw spectra and the solid line is the theoretical spectrum including the bandpass effects. The intensity of the theoretical spectrum is dictated by the need of avoiding undershoots below zero in the difference spectrum given by the open points. The nondispersive contributions (difference spectra) in cases 4 and 6 have the same shape and the same energy position as shown by the comparison in the middle panel, where they have been rescaled to the same height. In the further analysis we will represent the nondispersive contribution by the smooth interpolation (heavy solid line) given in the middle panel.

The shape of the nondispersive component summed over the polarizations has no evident connection with the occupied local density of $3d$ states (DOS) in the Mn site calculated in Ref. 13. This calculation is given in the upper panel of Fig. 6 (heavy line) after summing over the spin and after suitable broadening to compare with the present measurements (the thin line gives the empty DOS). Since we want to compare the shape of the calculated local DOS with the experiment, the position of the Fermi level is not critical and we have tentatively aligned the end points of the calculated DOS and of the experimental nondispersive component. In consideration of the completely different shape of the two curves, it seems very unlikely that matrix elements effects can solve the discrepancy. On the other hand, the calculations of Ref. 13 have been done with a method that gave good results in a variety of different $3d$ samples in agreement with photoemission as mentioned in the original reference (and in references quoted therein). Thus the present determination of the nondispersive component casts strong doubts upon the possibility of describing the $3d$ fluorescence of Mn impurities as DOS-like. Our results do not support a
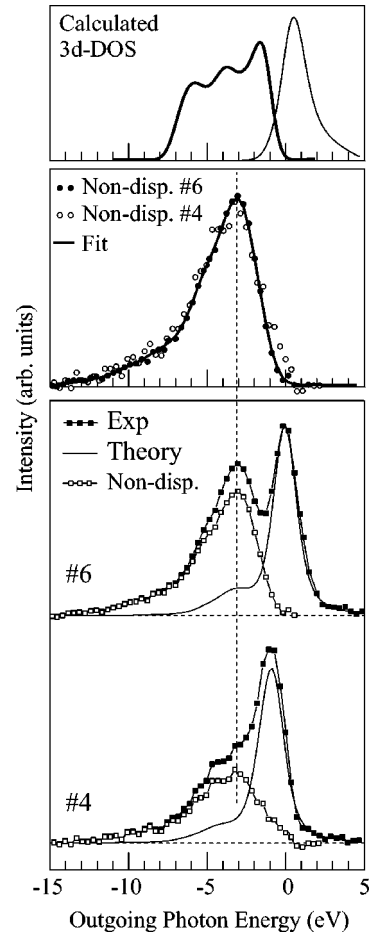

FIG. 6. Magnetic Mn impurities in Ni: determination of the nondispersive component in the emission spectra (cases 4 and 6), summed over the incident polarizations (the excitation energies are defined in the upper panel of Fig. 1). The thin lines in the lower panel give the theory. The extracted nondispersive components in cases 4 and 6 are compared in the middle panel. The theoretical $3d$ density of states in the Mn site summed over the spin (Ref. 13) are given in the upper panel after suitable broadening to compare with the experiment (the occupied states are given by the heavy line and empty states by the thin line).

straightforward interpretation of the nondispersive dichroism in terms of occupied spin unbalance (as in the initial suggestion by Strange *et al.*,[1] although this approach is acceptable in other cases[5] and has been considered as a possibility in magnetic compounds containing Mn, by Duda[8] and Yablonskikh *et al.*[9]). This calls for an assessment of the processes contributing to the nondispersive component and responsible for the departure from the DOS-like behavior. In general terms, the research on this problem in correlated systems is still under way and a variety of mechanisms has been suggested. The relaxation of the intermediate excited state with the creation of electron-hole pairs discussed in insulators[33,34] does not seem to be the best candidate for metals. A more promising approach is to consider the transfer of the excitation energy to the continuum due to the infinite dimension of the system.[35−37] In this connection, the model suggested in Ref. 36, accounting for all partitions of
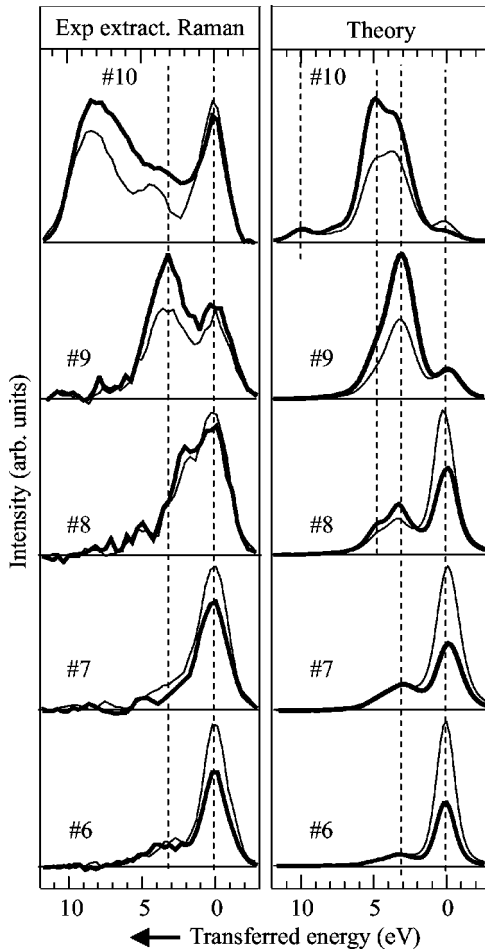
FIG. 7. Comparison between theory and experiment on magnetic Mn impurities in Ni with excitations from 6 to 10 specified in the upper panel of Fig. 1. The left column gives the extracted Raman spectra, i.e., the measurements after subtraction of the nondispersive part as explained in the text. The right column gives the theory including the effect of the experimental bandpass and of the partial polarization of the incident beam.

the excitation energy between localized and extended states during the excitation, seems promising. In fact, in other cases such as La metal[38] this model gives a good position of the nondispersive component, without using adjustable parameters. A calculation of this kind for a magnetic system is still lacking and could be stimulated by the present results.

The dispersive measurements (hereafter called "extracted Raman spectra") obtained from the raw measurements by subtracting the nondispersive components are compared with the calculations in Fig. 7. The theoretical simulations include the effect of the partial polarization of the incident beam and of the experimental bandpass in the incident and in the emitted photon beam.[39] The simulations do not include the effect of self-absorption/saturation that reduces the measured dichroism around the L_3 excitation with small effects on the other spectra (Sec. V).

If we neglect for the moment case 10, the comparison given in Fig. 7 shows a good general agreement between theory and experiment, as far as the trends and the spectral shape are concerned. This comparison deserves the following comments.

(i) The measured Raman peak dichroism in case 6 is 41%. The theoretical value is 73%, which has to be reduced to about 51% due to the self-absorption/saturation effect (see Sec. V). The two values compare well but the theory seems to give a somewhat larger dichroism. The same situation is seen in case 7 where the size of the theoretical dichroism is also somewhat greater. In case 9 the peak dichroism of the inelastic part is about 45% while the theoretical value is about 54% after the slight correction due to self-absorption/saturation. Again there is agreement but a larger dichroism is found in the calculations.

(ii) The spectra measured around the zero crossing of the absorption MCD (case 8) show opposite dichroism in the elastic and in the inelastic regions. This is seen both in the measurements and in the theory where the effect is much more evident. The handling of this spectrum is delicate and small details of the nondispersive part to be subtracted can affect the results. Thus we cannot discuss in detail this point. However, it is comfortable that there are similar qualitative trends in the theory and in the experiment.

(iii) The excitation 10 just below the L_2 threshold gives the widest spectrum free of the complications coming from the Coster-Kronig conversion. In this case, the theory predicts that the transferred energy scale becomes wider with a dominant loss at around 5 eV and a tiny feature at much greater transferred energy (at about 10 eV). In addition, in the experiment the energy scale is more expanded and perhaps the feature at 5 eV is seen. However, the general shape of the calculated spectrum is different from the experiment mainly concerning the intensity of the elastic peak. Moreover, there is no way of extracting a Raman spectrum in acceptable agreement with the theory at transferred energies greater than about 6 eV. In this region of the $(h\nu_{in}, h\nu_{out})$ plane a theory based on a single ion is thus not appropriate. In effect the model does not account for the charge fluctuations between the Mn ion and the environment including the Ni $3d$ derived states and the conduction band including the $4s$ contributions from Ni and from Mn impurities. In the reality these fluctuations can take place and might be the origin of the observed loss. Of course, this is only a conjecture deserving further investigation. In this energy region the situation is different with respect to $Ni_{75}Mn_{10}Al_{15}$ reported in Ref. 8 where it seems that there is only a nondispersive feature around -12 eV. This comparison cannot be done in more detail since the data on $Ni_{75}Mn_{10}Al_{15}$ as presented in Ref. 8 do not allow the correction due to self-absorption/saturation that is expected to be very important for the reasons discussed in Sec. V.

(iv) With $h\nu_{in}$ well below the L_3 threshold, both the experiment and the theory give a single Raman dispersing peak. This has essentially no inelastic tail, as shown by the raw data in case 2 of Fig. 1. Thus there is no need of extracting the Raman spectra and the theory agrees directly with the experiment. For space reasons, we do not give details on this point.

The limitations of the above treatment deserve some comment. The larger dichroism in the emission calculations

(typically by 25%) comes from the condition of fitting simultaneously the emission MCD and the absorption MCD. This shows the great importance of treating jointly the two sets of results. If this constraint is relaxed, it is relatively easy to obtain a better agreement with the emission measurements since it would suffice to increase the reduced temperature by using $T_R \approx 2.2$ in place of 1.5. However, this would give an absorption MCD not fully compatible with the experimental information. In this connection, a variety of problems could be investigated and this could stimulate further research. One point is to account for the noninteger occupation of the Mn-$3d$ shell. The ground-state calculations by Zeller[13] give an occupation of the Mn-$3d$ shell within the Wigner-Seitz sphere of 5.43 electrons which is roughly 10% greater than the 5 occupation assumed here. The trend towards an occupation greater than 5 is also found in Mn chemisorbed on Fe(100) accordingly to Ref. 30 (Mn-$3d$ occupation 5.23 from the $L_{2,3}$ absorption fitting). Moreover, also cluster calculations deserve to be explored mainly in connection with excitations well above L_3 (see the above discussion of excitation 10). However, all these treatments have probably to wait for an assessment of the more drastic approximation implicit in the whole work done up to now in emission dichroism, to the authors' knowledge. This is the assumption that the branching ratio to the Auger decay of the $L_{2,3}$ core hole with respect to radiative decay is polarization and energy independent. Only in this case it is legitimate to decouple the radiative and the Auger decays, by treating the photon scattering as it is done usually and as done here. If this is not the case, the dichroism seen in the photon channel can be influenced drastically by that in the Auger channel which is the dominant decay.[40] This argument is also supported by the unpolarized calculations on Ni of Ref. 21, showing that the branching ratio between Auger and radiative L_3 decay is not strictly independent on the excitation energy. The study of this problem (both experimentally and computationally) is probably the most stimulating perspective suggested by the present work. Its clarification could open an entirely new field to emission MCD.

VIII. CONCLUSIONS

We have presented a study of dichroic resonant emission spectroscopy excited with circularly polarized light at the $L_{2,3}$ thresholds of magnetic Mn impurities in Ni. This is a prototypical case of magnetic impurities, a field not yet explored with emission dichroism. We have shown that magnetic impurities are particularly convenient to this end, since most of the problems coming from self-absorption/saturation are eliminated. Consequently, the extraction of the relevant information from the measurements is much simpler and safer than in the other cases. The joint consideration of absorption MCD and emission MCD is greatly useful since it gives a further constraint in the theoretical fitting. The experimental information on absorption MCD has been obtained by the analysis of the specular reflectivity measured in the same experiment. We stress that it would have been impossible to calibrate the absorption MCD without the reflectivity measurements. The spectral components dispersing with the incident photon energy have been discussed in conjunction with multiplet splitting calculations in a simple ionic model with crystal field. Even in a metallic case as the present one, the model accounts for all measured trends with the exception of the excitation well above L_3 (i.e., just below L_2). The difference between the measurements and the dispersive theoretical spectra gives the nondispersive component already visible in the raw measurements. The shape of the nondispersive component has no evident correlation with the calculated ground electron states of Mn-$3d$ in Ni. This does not support a straightforward interpretation of the nondispersive component in terms of spin unbalance of the occupied states at variance with other cases present in the literature. The future implications, both theoretical and experimental, of the present results have also been discussed.

[1] P. Strange, P. J. Durham, and B. L. Gyorffy, Phys. Rev. Lett. **67**, 3590 (1991).

[2] C. F. Hague, J.-M. Mariot, P. Strange, P. J. Durham, and B. L. Gyorffy, Phys. Rev. B **48**, 3560 (1993).

[3] L.-C. Duda, J. Sthör, D. C. Mancini, A. Nilsson, N. Wassdahl, J. Nordgren, and M. G. Samant, Phys. Rev. B **50**, 16 758 (1994).

[4] C. F. Hague, J.-M. Mariot, G. Y. Guo, K. Hricovini, and G. Krill, Phys. Rev. B **51**, 1370 (1995).

[5] L. Braicovich, C. Dallera, G. Ghiringhelli, N. B. Brookes, and J. B. Goedkoop, Phys. Rev. B **55**, R14 729 (1997).

[6] S. Eisebitt, J. Lüning, J.-E. Rubensson, D. Schmitz, S. Blügel, and W. Eberhardt, Solid State Commun. **104**, 173 (1997).

[7] L. Braicovich, C. Dallera, G. Ghiringhelli, N. B. Brookes, and J. B. Goedkoop, Solid State Commun. **105**, 263 (1998).

[8] L.-C. Duda, J. Electron Spectrosc. Relat. Phenom. **110-111**, 287 (2000).

[9] M. V. Yablonskikh, V. I. Grebennikov, Yu. M. Yarmoshenko, E. Z. Kurmaev, S. M. Butorin, L.-C. Duda, C. Sathe, T. Käämbre, M. Magnuson, J. Nordgren, S. Plogmann, and M. Neumann, Solid State Commun. **117**, 79 (2001).

[10] When our paper was ready to be submitted a more extensive account of the results on Mn alloys given already in the present

Ref. 9 has been published: M. V. Yablonskikh, Yu. M. Yarmosh-enko, V. I. Grebennikov, E. Z. Kurmaev, S. M. Butorin, L.-C. Duda, J. Nordgren, S. Plogmann, and M. Neumann, Phys. Rev. B **63**, 235117 (2001). Since the basic messages are not changed in this new publication, our work on Mn impurities takes into account both contributions by M.V. Yablonskikh *et al.*

[11] T. Jo and J.-C. Parlebas, J. Phys. Soc. Jpn. **68**, 1392 (1999).

[12] This also implies that no correction to the raw data will be needed in experiments possible not too far from now.

[13] R. Zeller, J. Phys. F **17**, 2123 (1987).

[14] Some hints on the measurement of the outgoing polarization are given in Ref. 8.

[15] J. Goulon, N. B. Brookes, C. Gauthier, J. Goedkoop, C. Goulon-Ginet, M. Hagelstein, and A. Rogalev, Physica B **208-209**, 199 (1995).

[16] P. Elleaume, J. Synchrotron Radiat. **1**, 19 (1994).

[17] G. Ghiringhelli, A. Tagliaferri, L. Braicovich, and N. B. Brookes, Rev. Sci. Instrum. **69**, 1610 (1998).

[18] C. Dallera, E. Puppin, G. Trezzi, N. Incorvaia, A. Fasana, L. Braicovich, N. B. Brookes, and J. B. Goedkoop, J. Synchrotron Radiat. **3**, 231 (1996).

[19] C. Dallera, G. Ghiringhelli, and L. Braicovich, Rev. Sci. Instrum. **67**, 355 (1996).

[20] R. D. Cowan, *The Theory of Atomic Structure and Spectra* (University of California Press, Berkeley, 1981).

[21] F. M. F. de Groot, M. A. Arrio, Ph. Sainctavit, Ch. Cartier, and C. T. Chen, Solid State Commun. **92**, 991 (1994).

[22] S. M. Butorin, J.-H. Guo, M. Magnuson, P. Kuiper, and J. Nordgren, Phys. Rev. B **54**, 4405 (1996).

[23] In cases 10, 11, and 12 the spectrum is distributed in a wide energy range and in case 10 the scattering cross section is very low. Thus it has not been possible to obtain a statistics comparable to the other spectra as it is clear from Fig. 1. The spectra from cases 10 to 12 in Fig. 1 have roughly 50% more broadening since they have been numerically smoothed with a Gaussian convolution. This has no effect on the position of the main inelastic peak of spectrum 10.

[24] J. W. Cable and H. R. Child, Phys. Rev. B **10**, 4607 (1974).

[25] H. Akai and P. H. Dedrichs, Phys. Rev. B **47**, 8739 (1993).

[26] M. Sacchi and M. Mirone, Phys. Rev. B **57**, 8408 (1998).

[27] B. L. Henke, E. M. Gullikson, and J. C. Davis, At. Data Nucl. Data Tables **54**, 181 (1993).

[28] For example, an optimized experiment at the new beam line ID08 of the ESRF can probably go close to this ideal condition. This new beam line is supporting the first experiments starting from spring 2001.

[29] T. Böske, W. Clemens, C. Carbone, and W. Eberhardt, Phys. Rev. B **49**, 4003 (1994).

[30] J. Dresselhaus, D. Spanke, F. U. Hillebrecht, E. Kisker, G. van der Laan, J. B. Goedkoop, and N. B. Brookes, Phys. Rev. B **56**, 5461 (1997).

[31] M. C. Richter, P. Bencok, R. Brochier, V. Ilakovac, O. Heckmann, G. Paolucci, A. Goldoni, R. Larciprete, J.-J. Gallet, F. Chevrier, G. van der Laan, and K. Hricovini, Phys. Rev. B **63**, 205416 (2001).

[32] We have done also the calculation in the ''two-step model,'' where absorption and emission processes are decoupled, by neglecting the cross products in the development of the square modulus of Eq. (1). We only mention that the full calculation gives much better agreement with the experiment than this approximation, especially for the intensity of the elastic peak compared to the inelastic part. A detailed comparison between the exact calculation and the ''two-step'' model is beyond the scope of the present work and will be given elsewhere. This comparison for a simpler nonmagnetic case is done in F. M. F. de Groot, Phys. Rev. B **53**, 7099 (1996).

[33] L. Braicovich, C. Dallera, G. Ghiringhelli, N. B. Brookes, J. B. Goedkoop, and M. A. van Veenendaal, Phys. Rev. B **55**, R15 989 (1997).

[34] M. Finazzi, N. B. Brookes, and F. M. F. de Groot, Phys. Rev. B **59**, 9933 (1999).

[35] F. Gel'mukhanov and H. Ågren, Phys. Rev. B **57**, 2780 (1998).

[36] W. A. Caliebe, C.-C. Kao, J. B. Hastings, M. Taguchi, A. Kotani, T. Uozumi, and F. M. F. de Groot, Phys. Rev. B **58**, 13 452 (1998).

[37] T. Idé and A. Kotani, J. Phys. Soc. Jpn. **67**, 3261 (1998).

[38] M. Taguchi, L. Braicovich, G. Ghiringhelli, A. Tagliaferri, F. Borgatti, C. Dallera, K. Giarda, and N. B. Brookes, Phys. Rev. B **63**, 235113 (2001).

[39] The effect of the incident bandpass is a Gaussian convolution. The bandpass of the incident beam is accounted for in an exact way as done in L. Braicovich, M. Taguchi, F. Borgatti, G. Ghiringhelli, A. Tagliaferri, N. B. Brookes, T. Uozumi, and A. Kotani, Phys. Rev. B **63**, 245 115 (2001).

[40] L. Braicovich and G. Ghiringhelli, Phys. Rev. B **58**, 6688 (1998).